Determination of eddy-diffusivity in the lowermost stratosphere

Determination of eddy diffusivity in the lowermost stratosphere

M. I. Hegglin,[1] D. Brunner,[1] T. Peter,[1] J. Staehelin,[1] V. Wirth,[2] P. Hoor,[3] and H. Fischer[3]

Received 20 January 2005; revised 17 May 2005; accepted 6 June 2005; published 7 July 2005.

[1] We present a 2D-advection-diffusion model that simulates the main transport pathways influencing tracer distributions in the lowermost stratosphere (LMS). The model describes slow diabatic descent of aged stratospheric air, vertical (cross-isentropic) and horizontal (along isentropes) diffusion within the LMS and across the tropopause using equivalent latitude and potential temperature coordinates. Eddy diffusion coefficients parameterize the integral effect of dynamical processes leading to small scale turbulence and mixing. They were specified by matching model simulations to observed CO distributions. Interestingly, the model suggests mixing across isentropes to be more important than horizontal mixing across surfaces of constant equivalent latitude, shining new light on the interplay between various transport mechanisms in the LMS. The model achieves a good description of the small scale tracer features at the tropopause with squared correlation coefficients R^2 = 0.72...0.94. **Citation:** Hegglin, M. I., D. Brunner, T. Peter, J. Staehelin, V. Wirth, P. Hoor, and H. Fischer (2005), Determination of eddy diffusivity in the lowermost stratosphere, *Geophys. Res. Lett.*, *32*, L13812, doi:10.1029/2005GL022495.

1. Introduction

[2] Tracer distributions influence ozone photochemistry and the radiative heating budget of the lowermost stratosphere (LMS). As indicated in Figure 1 they are affected by (1) large-scale diabatic sinking in the Brewer-Dobson circulation, (2) transport within the tropically controlled transition region (380 K < Θ < 450 K), and (3,4) two-way mixing across the tropopause and within the LMS [*Holton et al.*, 1995]. Troposphere-to-stratosphere transport (TST) in the extratropics is thought to occur mainly quasi-horizontally (process 3) along isentropes [*Chen*, 1995] in a process commonly referred to as 2D turbulence which is initiated by Rossby wave breaking events. Conversely, upward transport in the vertical, i.e. across isentropic surfaces (process 4), appears to be less important due to the stable vertical layering of the LMS. However, due to their small scales and episodic nature the potential of clear air turbulence, deep convection, and transient radiative heating events remains uncertain. Attempts to estimate TST by trajectory studies or chemical transport models suffer from the neglect of diabatic small-scale processes or from numerical diffusion, respectively [*Bourqui*, 2004, and references therein].

[3] Here we present a model describing the tracer fields in the LMS that ties in with the classical work of *Brewer* [1949]. It considers slow diabatic descent of air from the stratospheric overworld and approximates the integral effect of any processes causing small scale turbulence and mixing at the tropopause and within the LMS by vertical and horizontal eddy diffusion. The model simulations are compared to tracer distributions measured during eight seasonally conducted aircraft campaigns within the project SPURT [*Hegglin et al.*, 2004; *Hoor et al.*, 2004]. By matching model simulations to fit best the observed tracer time series, diffusion coefficients valid for the LMS-region were derived.

2. Model Description

[4] By the use of vorticity-based equivalent latitude (ϕ_e) as horizontal and potential temperature (θ) as vertical coordinate, the model is able to effectively reduce the complexity of tracer distributions by removing the effects of adiabatic excursions of air masses [*Butchart and Remsberg*, 1986] which lead to wave-like deformations of the tropopause in geographical space such as indicated in Figure 1a. In (ϕ_e, θ) coordinates (Figure 1b) an air parcel remains at a fixed location in the case of purely adiabatic and frictionless transport as both PV and θ are conserved simultaneously. The zonal coordinate can be neglected since zonal winds act to remove longitudinal gradients in tracer distributions.

[5] Figure 1b is a sketch of the basic processes described in the model. The 2D model domain spans the LMS and upper troposphere (270–420 K) with a resolution of 1° in the horizontal and 1 K in the vertical. Integration of the advection-diffusion equation (see equation (1) below) is only performed in the LMS whereas in the upper troposphere the concentration is fixed to a value χ_T which optionally varies with latitude. The position of the tropopause is kept constant during a model integration and the tropospheric concentration at the tropopause serves as lower boundary condition. The tropopause is defined as the 2 PVU surface corresponding to a unique value of ϕ_e on each θ-level. The upper model boundary is the 420 K isentrope where the concentration is fixed to a value χ_S which is influenced by processes 1 and 2 in Figure 1. In the tropics a transition zone is specified between 380 K and 420 K with χ decreasing linearly from χ_T to χ_S.

[6] Transport is described by the advection-diffusion equation

$$\frac{\partial \chi}{\partial t} = -\dot{\Theta}\frac{\partial \chi}{\partial \Theta} + \tilde{\nabla}^2 \chi + S, \qquad (1)$$

which is integrated to a steady state. Here, $\dot{\Theta}$ is the velocity of the large-scale diabatic downward motion (in Kelvin per day), and S is the net effect of chemical reactions. The

[1]Institute for Atmospheric and Climate Science, ETH Zurich, Switzerland.
[2]Institute for Atmospheric Physics, University of Mainz, Mainz, Germany.
[3]Max Planck Institute for Chemistry, Mainz, Germany.

0094-8276/05/2005GL022495

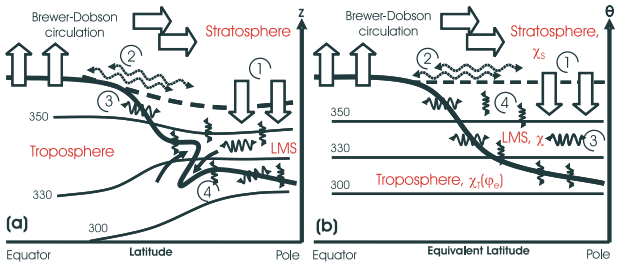

Figure 1. Dynamical aspects of TST, (a) in latitude/height coordinates, (b) in equivalent latitude/potential temperature coordinates. Thick line: dynamical tropopause (PV = 2), dashed line: 380 K isentrope, thin lines: lower isentropes. Processes: (1) diabatic descent, (2) transport within the tropically controlled layer, (3) quasi-horizontal mixing and (4) vertical mixing across the tropopause and within the stratosphere. The stratospheric intrusion in (a) is subsumed by the coordinates in (b). $\chi_T(\phi_e)$, χ_S, and χ indicate tracer mixing ratios in the troposphere, the stratosphere above 420 K, and the LMS (see text for details).

modified Laplace operator ($\tilde{\nabla}^2$) in spherical coordinates describes horizontal and vertical diffusion and is given by

$$\tilde{\nabla}^2 = k_{\Theta\Theta}\frac{\partial^2}{\partial\Theta^2} + k_{yy}\frac{1}{r^2\cos\phi_e}\frac{\partial}{\partial\phi_e}\left(\cos\phi_e\frac{\partial}{\partial\phi_e}\right), \qquad (2)$$

where $k_{\Theta\Theta}$ and k_{yy} are the vertical and horizontal eddy diffusion coefficients with units $K^2\ s^{-1}$ and $m^2\ s^{-1}$, respectively, r is the Earth radius. The eddy diffusion coefficients k_{yy} and $k_{\Theta\Theta}$ parameterize the integral effect of a variety of processes leading to mixing including filamentation (stretching and thinning), diabatic changes in PV through transient radiative processes, deep convective events reaching into the LMS, clear air turbulence, stirring and turbulence caused by breaking Rossby or gravity waves. Eddy diffusion and mean advection are considered to be unrelated.

[7] The advection term $\dot{\Theta}$ (i.e., the diabatic heating rate) was determined for every season by calculating the change in θ along a total of 145800 1-day forward trajectories started on three different days selected within the 10-day period before the flights and from a regular grid spanning the northern hemisphere with 2 × 2 degrees horizontal and 20 K vertical resolution between 300 and 400 K. The corresponding wind fields were taken from operational ECMWF analyses. Zonal means were calculated for the different vertical levels and these were again averaged to obtain one advection rate with only latitudinal dependency on which we applied a 3 point running mean to reduce variability in the meridional direction. They are strongest in autumn/winter with values around $-1.4\ K\ d^{-1}$ and weakest in summer with values around $-0.8\ K\ d^{-1}$.[1]

3. Results and Discussion

3.1. Determination and Seasonality of Diffusion Coefficients

[8] We have applied our model to CO, which is a tracer with a stratospheric lifetime of about three months exhibiting a strong gradient across the tropopause and which was measured with very high accuracy [*Hoor et al.*, 2004]. Chemistry (term S in Equation (1)) includes the source of CO (oxidation of CH_4 by OH) and the sink (oxidation of CO by OH). OH mixing ratios vary with hours of sunlight available depending on latitude and day of the year. The tropospheric and stratospheric CO background mixing ratios were obtained by averaging the SPURT measurements in the troposphere and by extrapolating the measurements on highest θ levels to 420 K, respectively. The diffusion coefficients were specified by matching model simulations to obtain the best fit for the observed CO values. The ability of the model to reproduce the CO measurements was quantified using a skill score $s = (1 + R)^2/(\hat{\sigma} + 1/\hat{\sigma})^2$, where R is the correlation coefficient and $\hat{\sigma} = \sigma_{model}/\sigma_{meas}$ is the normalized standard deviation. This formulation of a skill score accounts for both the correlation and the root mean square error between modeled and the measured CO values [*Taylor*, 2001].

[9] Figure 2 shows the CO values from three different simulations with varying k_{yy} and $k_{\Theta\Theta}$ interpolated to the (ϕ_e, θ) coordinates of a flight in spring 2003 together with the measurements. In absence of vertical and horizontal diffusion, the LMS is filled with the stratospheric background mixing ratio and a stepwise increase occurs at the tropopause. Adding diffusion in both, horizontal and vertical directions diminishes the gradient at the tropopause and produces CO values showing similar features as the observations at both large and small scales. The small-scale features are often associated with undulations in measured potential temperature (to which the model values are interpolated) and are most probably caused by gravity waves. For comparison the time series of PV along the flight track is also shown in Figure 2 (light grey line) suggesting a tight relationship with the observed CO mixing ratios. This is not to be expected a priori since on time scales of weeks to months corresponding to the diabatic circulation (represented by $\dot{\Theta}$ in our model) the relation may gradually weaken due to diabatic and chemical processes which have different effects on PV and chemical tracers, respectively

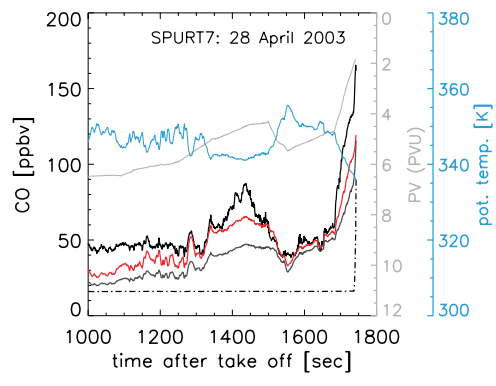

Figure 2. Influence of different diffusion coefficients on modeled CO along a SPURT flight in spring 2003. Measured CO: black line. Modeled CO: for $k_{yy} = 0$ and $k_{\Theta\Theta} = 0$ black dashed-dotted, for $k_{yy} = 3 \times 10^5\ m^2\ s^{-1}$ and $k_{\Theta\Theta} = 0$ dark grey, and for $k_{yy} = 0$ and $k_{\Theta\Theta} = 1 \times 10^{-4}\ K^2\ s^{-1}$ red line. PV and potential temperature along the flight: upper light grey and blue curves.

[1] Auxiliary material is available at ftp://ftp.agu.org/apend/gl/2005GL022495.

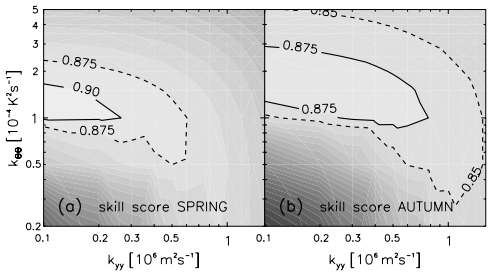

Figure 3. Skill score distributions (ability to model SPURT CO measurements) for (a) spring and (b) autumn as a function of k_{yy} and $k_{\Theta\Theta}$. Black solid and dotted lines delimit areas of highest skill score values, grey-tone covers values from 0.2 (dark) to 0.95 (light).

[*Haynes and McIntyre*, 1987]. Our model suggests that this relation is, at least partly, coincidental [cf. *Legras et al.*, 2003]: the combined effect of diabatic sinking and eddy mixing results in a tracer distribution which just happens to be similar to that of PV. PV in turn increases towards the poles due to the effect of the earth rotation and with altitude due to decreasing density.

[10] In order to determine the best vertical and horizontal diffusion coefficients the model has been run with a set of different k_{yy} and $k_{\Theta\Theta}$ for different seasons. The resulting skill score distributions for autumn 2002 and spring 2003 are shown in Figure 3. There is a relatively flat distribution of the skill scores, and interestingly the parameterization with $k_{\Theta\Theta}$ alone yields best results.

[11] The vertical diffusion coefficients in spring and autumn correspond to values between 0.45 and 0.65 m^2 s^{-1} and between 0.65 and 1.1 m^2 s^{-1}, respectively (assuming a uniformly distributed potential temperature gradient of 15 K km^{-1} in the LMS). The diffusion coefficients directly depend on the chosen diabatic heating rates and a given uncertainty in the latter may also produce the largest uncertainty in our estimates. Comparison with diffusion coefficients derived by *Legras et al.* [2003] valid for the same altitude range show that they are by at least a factor of 4 smaller than ours. This difference is partly caused by the applied values for $\Delta\Theta/\Delta z$.

[12] Assuming horizontal (isentropic) diffusion only, best agreement is obtained for a diffusion coefficient of the order of 1×10^6 m^2 s^{-1}. This value may be compared with estimates of 'effective diffusivity' as presented by *Haynes and Shuckburgh* [2000] for the same region being of the same order of magnitude. However, their approach only considers isentropic mixing whereas the CO tracer fields used for our estimates appear to be affected by cross-isentropic mixing also, since simulations with only horizontal mixing are unable to produce optimal results (see Figure 3).

3.2. CO Tracer Distribution

[13] The diffusion coefficients of the model run with the highest skill score are used for more qualitative evaluations. In Figure 4a the mean CO distribution obtained from the SPURT autumn campaign in 2002 is shown. The tracer distribution reveals a relatively simple behaviour when using (ϕ_e, θ) coordinates as shown by *Hoor et al.* [2004]. Measured CO mixing ratios closely follow the shape of the tropopause decreasing rapidly with increasing distance in $\Delta\Theta$ from the tropopause. However, CO isopleths and PV isolines are not strictly parallel. The gradient in the tracer mixing ratio is strongest at the tropopause but tropospheric influence reaches up to highest flight levels.

[14] Figure 4b then shows the CO distribution obtained in a model simulation for the same month. The model reproduces the main characteristics of the mean distribution of CO measured during the SPURT autumn campaign showing roughly exponentially decreasing mixing ratios with 'distance' from the tropopause. It establishes a smooth transition layer between the troposphere and the stratosphere within the LMS with strongest mixing ratio gradients close to the tropopause.

3.3. Comparison With Measured CO Time Series

[15] Figure 5 shows comparisons between simulated and measured CO time series of different SPURT flights in spring 2003 and autumn 2002. It illustrates the general applicability of a model simulation with optimized diffusion coefficients to reproduce every flight of the corresponding campaign. The simulations agree well with the main features of the observed tracer time series and in particular the observed tracer gradients at the tropopause. Even some smaller scale features are reproduced. Deviations may be partly due to errors in the PV field used for calculating ϕ_e along the flight track which is for instance expected in filaments not resolved by the ECMWF model. An improvement could be achieved by calculating ϕ_e out of PV values determined by the reverse domain filling (RDF) technique, which is known to reproduce sub-synoptic scale structures that are also seen in observational data [*Hegglin et al.*, 2004].

4. Conclusions

[16] The seasonal distributions of CO in the LMS in autumn and spring and complex structures observed along individual flights were successfully simulated by a simple 2D model using the main components of atmospheric transport, diabatic advection of air from the stratospheric overworld as well as horizontal and vertical eddy diffusion

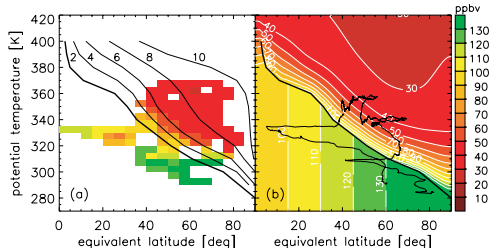

Figure 4. CO mixing ratio in (ϕ_e, θ) coordinates. (a) Mean CO mixing ratios in ppbv measured during the SPURT campaign in autumn 2002. Black lines denote isolines of potential vorticity. (b) CO distribution calculated by the model with $k_{yy} = 2 \times 10^5$ m^2 s^{-1} and $k_{\Theta\Theta} = 2.5 \times 10^{-4}$ K^2 s^{-1}. The tropospheric and stratospheric backgrounds were fixed to $\chi_T = \phi_e/2 + 90$ ppbv and $\chi_S = 30$ ppbv, respectively. The thick black line is the tropopause. White lines are contours of constant CO in ppbv, the thin black line exemplarily shows the path of a single flight.

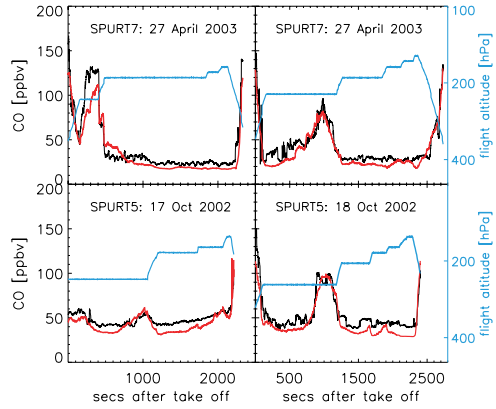

Figure 5. Comparisons between CO time series (black) obtained during the SPURT spring 2003 and autumn 2002 campaigns and from model simulations of the corresponding seasons (red). Diffusion coefficients, tropospheric and stratospheric background values used for spring were $k_{yy} = 0$, $k_{\Theta\Theta} = 1.5 \times 10^{-4}$ K^2 s^{-1}, $\chi_T = \phi_e/3 + 120$ ppbv, and $\chi_S = 15$ ppbv, and for autumn $k_{yy} = 2 \times 10^5$ m^2 s^{-1}, $k_{\Theta\Theta} = 2 \times 10^{-4}$ K^2 s^{-1}, $\chi_T = \phi_e/2 + 90$ ppbv, and $\chi_S = 30$ ppbv. Blue line indicates the flight path.

within the LMS and across the tropopause. Fitting model simulations towards aircraft measurements of CO was used to determine eddy diffusion coefficients for the LMS which parameterize different sub-grid processes leading to mixing of air masses. The strength of the model lies in the applied coordinate system of equivalent latitude and potential temperature, that simplifies the complexity of transport processes within the atmosphere.

[17] Simulated tracer mixing ratios are highly correlated with observed ones (R^2 between 0.72 and 0.94). The high correlation is dominated by flight sections crossing the strong tracer gradients close to the tropopause reflected simultaneously in large variations in PV. Small scale structures on the other hand are determined by fluctuations in potential temperature [cf. *Sparling and Bacmeister*, 2001].

[18] The diffusion coefficients deduced from measurements of a spring and an autumn campaign indicate a seasonal dependency with higher values in autumn than spring. The slightly higher diffusivity in autumn is in accordance with a stronger wave activity in this season (and an enhanced mean meridional circulation). Surprisingly, mixing across isentropes appears to be more important than mixing along isentropic surfaces which has been exclusively investigated in many previous studies.

[19] The presented model offers an integrated and simplified view of tracer transport at the extratropical tropopause. It demonstrates the importance of diabatic mixing across surfaces of constant θ and/or PV to balance the diabatic sinking of CO poor air from the overworld. The two counteracting processes result in a smooth transition layer between troposphere and stratosphere with a strong tracer gradient in the first 20 K above the local tropopause. Diabatic mixing is driven by recurrent wave-breaking events in the tropopause region that produce filaments of tropospheric air traveling into the stratosphere and vice versa, bringing air masses with different chemical and radiative characteristics into close proximity. Small-scale processes such as three-dimensional turbulence and ultimately molecular diffusion then act to reduce these inhomogeneities. Considering the vertical to horizontal aspect ratio of such filamentary structures, the chemical, dynamical and radiative gradients are stronger in the vertical than in the horizontal and hence mixing may also be more efficient in the vertical. This is suggested by the model results showing a substantial improvement in simulated tracer distributions when vertical eddy-diffusion is included in the model (process 4 in Figure 1).

[20] The derived diffusion coefficients should be further validated by the use of other long-lived tracer data sets with broader spatial and temporal coverage. The model then provides a possibility to define the partitioning between tropospheric and stratospheric air in the LMS with lowest calculation efforts.

[21] **Acknowledgments.** We thank the Swiss National Fund (SNF) for financial support, ECMWF and MeteoSwiss for meteorological analysis data. We are grateful to Peter Haynes (Cambridge), Ted Shepherd (Toronto), Zhiming Kuang and Marcia Baker (Seattle) for helpful discussions.

References

Bourqui, M. (2004), Stratosphere-troposphere exchange from the Lagrangian perspective: A case study and method sensitivities, *Atmos. Chem. Phys.*, *4*, 3249–3284.

Brewer, A. (1949), Evidence for a world circulation provided by the measurements of helium and water vapor distribution in the stratosphere, *Q. J. R. Meteorol. Soc.*, *75*, 351–363.

Butchart, N., and E. E. Remsberg (1986), The area of the stratospheric polar vortex as a diagnostic for tracer transport on an isentropic surface, *J. Atmos. Sci.*, *43*(13), 1319–1339.

Chen, P. (1995), Isentropic cross tropopause mass exchange in the extratropics, *J. Geophys. Res.*, *100*, 16,661–16,673.

Haynes, P. H., and M. E. McIntyre (1987), On the evolution of vorticity and potential vorticity in the presence of diabatic heating and frictional or other forces, *J. Atmos. Sci.*, *44*(5), 828–841.

Haynes, P., and E. Shuckburgh (2000), Effective diffusivity as a diagnostic of atmospheric transport: 2. Troposphere and lower stratosphere, *J. Geophys. Res.*, *105*, 22,795–22,810.

Hegglin, M. I., et al. (2004), Tracing troposphere to stratosphere transport within a mid-latitude deep convective system, *Atmos. Chem. Phys.*, *4*, 741–756.

Holton, J., P. Haynes, M. McIntyre, A. Douglass, R. Rood, and L. Pfister (1995), Stratosphere-troposphere exchange, *Rev. Geophys.*, *33*, 403–439.

Hoor, P., C. Gurk, D. Brunner, M. I. Hegglin, H. Wernli, and H. Fischer (2004), Seasonality and extent of extratropical TST derived from in-situ CO measurements during SPURT, *Atmos. Chem. Phys.*, *4*, 1691–1726.

Legras, B., B. Joseph, and F. Lefevre (2003), Vertical diffusivity in the lower stratosphere from Lagrangian back-trajectory reconstructions of ozone profiles, *J. Geophys. Res.*, *108*(D18), 4562, doi:10.1029/2002JD003045.

Sparling, L. C., and J. T. Bacmeister (2001), Scale dependence of tracer microstructure: PDFs, intermittency and the dissipation scale, *Geophys. Res. Lett.*, *28*, 2823–2826.

Taylor, K. E. (2001), Summarizing multiple aspects of model performance in a single diagram, *J. Geophys. Res.*, *106*, 7183–7192.

D. Brunner, M. I. Hegglin, T. Peter, and J. Staehelin, IACETH, Universitaetsstr. 16, 8092 Zurich, Switzerland. (michaela.hegglin@alumni.ethz.ch)

H. Fischer and P. Hoor, Max Planck Institute for Chemistry, D-55020 Mainz, Germany.

V. Wirth, Institute for Atmospheric Physics, University of Mainz, D-55099 Mainz, Germany.